

Quantum computing with electrical circuits: Hamiltonian construction for basic qubit-resonator models

Michael R. Geller

Department of Physics and Astronomy, University of Georgia, Athens, Georgia 30602, USA

June 4, 2007

Abstract

Recent experiments motivated by applications to quantum information processing are probing a new and fascinating regime of electrical engineering—that of quantum electrical circuits—where macroscopic collective variables such as polarization charge and electric current exhibit quantum coherence. Here I discuss the problem of constructing a quantum mechanical Hamiltonian for the low-frequency modes of such a circuit, focusing on the case of a superconducting qubit coupled to a harmonic oscillator or resonator, an architecture that is being pursued by several experimental groups.

1 Quantum gate design

In the quantum circuit model of quantum information processing, an arbitrary unitary transformation on N qubits can be decomposed into a sequence of certain universal two-qubit logical operations acting on pairs of qubits, combined with arbitrary single-qubit rotations [1]. The purpose of quantum gate design is to develop experimental protocols or “machine language code” to implement these elementary operations.

For quantum information processing architectures based on superconducting circuits [2, 3], the first step is to construct an effective Hamiltonian for the system. Whereas the fully microscopic Hamiltonian for the electronic and ionic degrees of freedom in the conductors forming the circuit is known, at least in principle, the Hamiltonian of interest here describes only the relevant low-energy modes of that circuit.

A rigorous construction might involve making a canonical transformation from the microscopic quantum degrees of freedom to a set of collective modes. Here I follow a simpler and more intuitive phenomenological quantization method, whereby a classical description based on Kirchoff’s laws is derived first, and then later canonically quantized. It is important to realize that such an approach is not based on first principles and must be confirmed experimentally.

2 The phase qubit

The primitive building block for any superconducting qubit is the Josephson junction (JJ) shown in Fig. 1. The low-energy dynamics of this system is governed by the phase difference φ between the condensate wave functions or order parameters on the two sides of the insulating barrier. The phase difference is an operator canonically conjugate to the Cooper-pair number difference N , according to¹

$$[\varphi, N] = i. \quad (1)$$

The low-energy eigenstates $\psi_m(\varphi)$ of the JJ can be regarded as probability-amplitude distributions in φ . As will be explained below, the potential energy $U(\varphi)$ of the JJ is manipulated by applying a bias current I to the junction, providing an external control of the quantum

¹We define the momentum P to be canonically conjugate to φ , and $N \equiv P/\hbar$. In the phase representation, $N = -i\frac{\partial}{\partial\varphi}$.

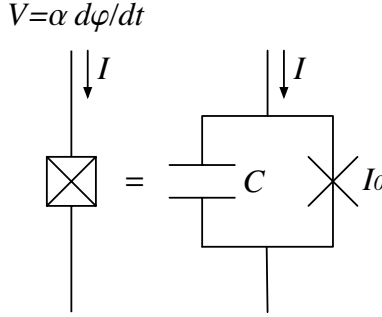


Figure 1: Circuit model for a current-biased JJ, neglecting dissipation. Here $\alpha \equiv \hbar/2e$.

states $\psi_m(\varphi)$, including the qubit energy-level spacing ϵ . The crossed box in Fig. 1 represents a “real” JJ. The cross alone represents a nonlinear element that satisfies the Josephson equations²

$$I = I_0 \sin \varphi \quad \text{and} \quad V = \alpha \dot{\varphi}, \quad (2)$$

with critical current I_0 . The capacitor accounts for junction charging.³ A single JJ is characterized by two energy scales, the Josephson coupling energy

$$E_J \equiv \frac{\hbar I_0}{2e}, \quad (3)$$

where e is the magnitude of the electron charge, and the Cooper-pair charging energy

$$E_c \equiv \frac{(2e)^2}{2C}, \quad (4)$$

with C the junction capacitance. For example,

$$E_J = 2.05 \text{ meV} \times I_0[\mu\text{A}] \quad \text{and} \quad E_c = \frac{320 \text{ neV}}{C[\text{pF}]}, \quad (5)$$

where $I_0[\mu\text{A}]$ and $C[\text{pF}]$ are the critical current and junction capacitance in microamperes and picofarads, respectively. In the regimes of interest to quantum computation, E_J and E_c are assumed to be larger than the thermal energy $k_B T$ but smaller than the superconducting energy gap Δ_{sc} , which is about $180 \mu\text{eV}$ in Al. The relative size of E_J and E_c vary, depending on the specific qubit implementation.

The basic phase qubit considered here consists of a JJ with an external current bias, and is shown in Fig. 2. The classical Lagrangian for this circuit is

$$L_{\text{JJ}} = \frac{1}{2} M \dot{\varphi}^2 - U, \quad M \equiv \frac{\hbar^2}{2E_c}. \quad (6)$$

Here

$$U \equiv -E_J (\cos \varphi + s \varphi), \quad \text{with} \quad s \equiv \frac{I}{I_0}, \quad (7)$$

² $\alpha \equiv \hbar/2e$.

³This provides a simple mean-field treatment of the *inter*-condensate electron-electron interaction neglected in the standard tunneling Hamiltonian formalism on which the Josephson equations are based.

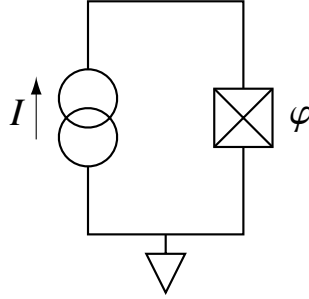


Figure 2: Basic phase qubit circuit.

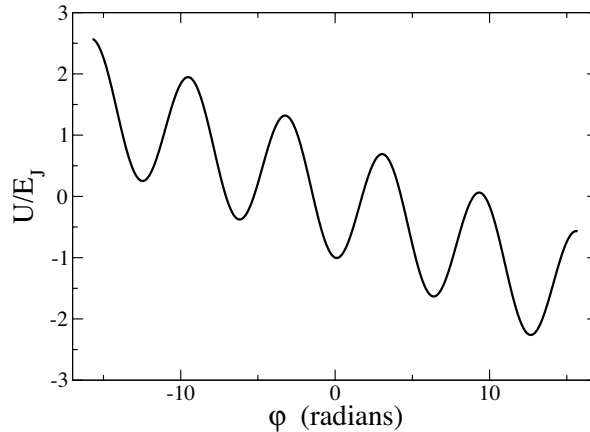


Figure 3: Effective potential for a current-biased JJ. The slope of the cosine potential is s . The potential is harmonic for the qubit states unless s is very close to 1.

is the effective potential energy of the JJ, shown in Fig. 3. Note that the “mass” M in (6) actually has dimensions of mass \times length². The form (6) results from equating the sum of the currents flowing through the capacitor and ideal Josephson element to I . The phase qubit implementation uses $E_J \gg E_c$.

According to the Josephson equations, the classical canonical momentum $P = \frac{\partial L}{\partial \dot{\varphi}}$ is proportional to the charge Q or to the number of Cooper pairs $Q/2e$ on the capacitor according to $P = \hbar Q/2e$. The quantum Hamiltonian can then be written as

$$H_{JJ} = E_c N^2 + U, \quad (8)$$

where φ and N are operators satisfying (1). Because U depends on s , which itself depends on time, H_{JJ} is generally time-dependent. The low lying stationary states when $s < 1$ are shown in Fig. 4. The two lowest eigenstates $|0\rangle$ and $|1\rangle$ are used to make a qubit. ϵ is the level spacing and ΔU is the height of the barrier.

A useful “spin $\frac{1}{2}$ ” form of the phase qubit Hamiltonian follows by projecting (8) to the qubit subspace. There are two natural ways of doing this. The first is to use the basis of the

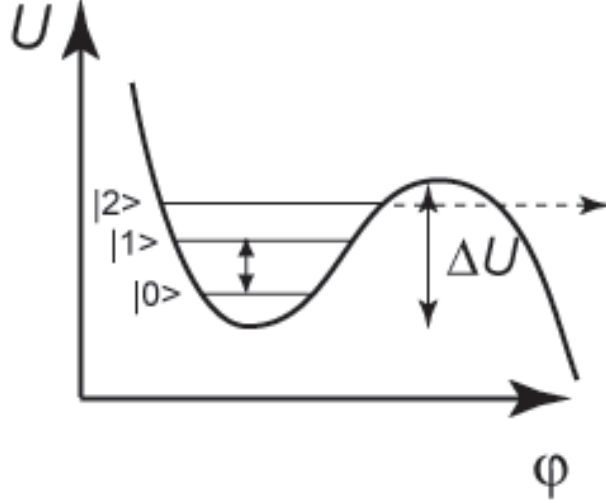


Figure 4: Effective potential in the anharmonic regime, with s very close to 1. State preparation and readout are carried out in this regime.

s -dependent eigenstates, in which case

$$H = -\frac{\hbar\omega_p}{2} \sigma^z, \quad (9)$$

where

$$\omega_p \equiv \omega_{p0}(1 - s^2)^{\frac{1}{4}} \quad \text{and} \quad \omega_{p0} \equiv \sqrt{2E_c E_J}/\hbar. \quad (10)$$

The s -dependent eigenstates are called instantaneous eigenstates, because s is usually changing with time. The time-dependent Schrödinger equation in this basis contains additional terms coming from the time-dependence of the basis states themselves, which can be calculated in closed form in the harmonic limit [4]. These additional terms account for all nonadiabatic effects.

The second spin form uses a basis of eigenstates with a fixed value of bias, s_0 . In this case

$$H = -\frac{\hbar\omega_p(s_0)}{2} \sigma^z - \frac{E_J \ell}{\sqrt{2}} (s - s_0) \sigma^x, \quad (11)$$

where

$$\ell \equiv \ell_0(1 - s_0)^{-\frac{1}{8}} \quad \text{and} \quad \ell_0 \equiv \left(\frac{2E_c}{E_J} \right)^{\frac{1}{4}}. \quad (12)$$

This form is restricted to $|s - s_0| \ll 1$, but it is very useful for describing rf pulses.

The angle ℓ characterizes the width of the eigenstates in φ . For example, in the s_0 -eigenstate basis (and with s_0 in the harmonic regime), we have

$$\varphi = \varphi_{01} \sigma^x + \arcsin(s_0) I, \quad \text{with} \quad \varphi_{mm'} \equiv \langle m | \varphi | m' \rangle. \quad (13)$$

Here $\varphi_{mm'}$ is an effective dipole moment (with dimensions of angle, not length), and $\varphi_{01} = \ell/\sqrt{2}$.

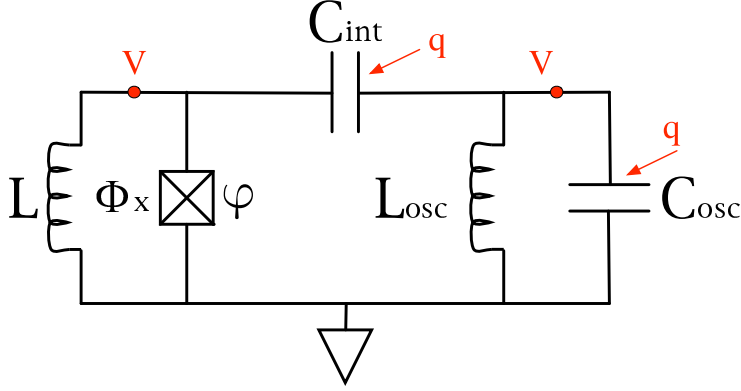


Figure 5: Circuit model for a superconducting qubit coupled to a parallel LC oscillator.

3 Qubit-oscillator models

Circuit diagrams for an rf squid capacitively coupled to parallel and series LC oscillators are shown in Figs. 5 and 6. Φ_x is an external flux bias, and φ is the phase difference across the JJ (the phase of the ungrounded superconductor relative to the grounded side is φ). Quantization of the total magnetic flux Φ in the squid loop leads to the condition (in cgs units)

$$\Phi = \Phi_x - cLI = \Phi_{\text{sc}} \frac{\varphi}{2\pi}, \quad \Phi_{\text{sc}} \equiv \frac{hc}{2e} \quad (14)$$

where I is the current flowing downward through the Josephson junction, related to φ by

$$\alpha C \ddot{\varphi} + I_0 \sin \varphi = I. \quad (15)$$

Here C and I_0 are the usual JJ capacitance and critical-current parameters, and

$$\alpha \equiv \frac{\hbar}{2e}. \quad (16)$$

The minus sign in (14) reflects the diamagnetic (for $0 < \varphi < \pi$) screening by the superconducting loop. The quantization condition (14) assumes an isolated squid (specifically, that no current is being provided by the coupling capacitor). In Figs. 5 and 6 the voltage across the JJ is

$$V = \alpha \dot{\varphi}. \quad (17)$$

3.1 JJ coupled to parallel LC oscillator

Referring to Fig. 5, the equations of motion for φ and q are

$$\alpha^2 (C + C_{\text{int}}) \ddot{\varphi} + E_J \sin \varphi + \frac{\alpha \Phi_{\text{sc}}}{2\pi cL} \varphi - \frac{\alpha \Phi_{\text{ext}}}{cL} = \alpha \frac{C_{\text{int}}}{C_{\text{osc}}} \dot{q} \quad (18)$$

and

$$L_{\text{osc}} \left(1 + \frac{C_{\text{int}}}{C_{\text{osc}}} \right) \ddot{q} + \frac{q}{C_{\text{osc}}} = \alpha L_{\text{osc}} C_{\text{int}} \ddot{\varphi}. \quad (19)$$

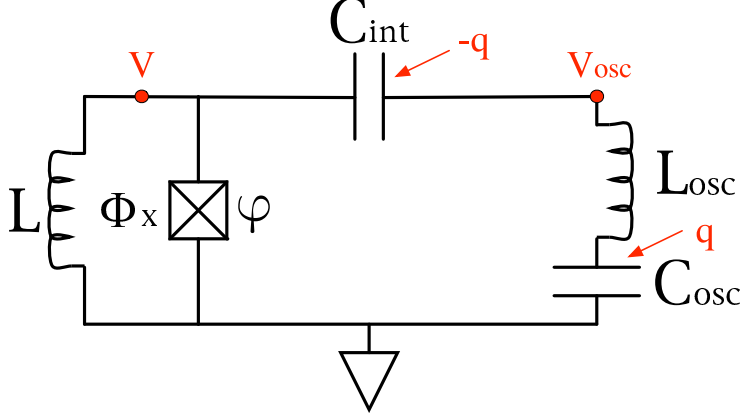


Figure 6: Circuit model for qubit coupled to series LC oscillator.

Surprisingly, it is not possible to find a Lagrangian (local in time and a polynomial in $\frac{d^m \varphi}{dt^m}$ and $\frac{d^n q}{dt^n}$) that gives these equations of motion. To proceed, we make a transformation from q to a dimensionless node-flux variable ϕ , defined as

$$\phi(t) \equiv \frac{1}{\alpha C_{\text{osc}}} \int_{-\infty}^t q(t') dt', \quad (20)$$

use $q = \alpha C_{\text{osc}} \dot{\phi}$, and integrate the equation resulting from (19) over time. This leads to the coupled equations

$$\alpha^2 (C + C_{\text{int}}) \ddot{\varphi} + E_J \sin \varphi + \frac{\alpha^2}{L} \varphi - \frac{2\pi \alpha^2 x}{L} = \alpha^2 C_{\text{int}} \ddot{\phi} \quad (21)$$

and

$$\alpha^2 (C_{\text{osc}} + C_{\text{int}}) \ddot{\phi} + \frac{\alpha^2}{L_{\text{osc}}} \phi = \alpha^2 C_{\text{int}} \ddot{\varphi} + \text{const}, \quad (22)$$

where

$$x \equiv \frac{\Phi_x}{\Phi_{\text{sc}}} \quad (23)$$

is the dimensionless flux bias. The integration constant in (22) acts as an applied static force and can be dropped (corresponding to a shift in ϕ). Note the symmetry in the cross-coupling terms on the right-hand-sides of (21) and (22).

A Lagrangian leading to (21) and (22) is

$$L = \frac{\alpha^2 C}{2} \dot{\varphi}^2 + E_J \cos \varphi - \frac{\alpha^2}{2L} (\varphi - 2\pi x)^2 + \frac{\alpha^2 C_{\text{osc}}}{2} \dot{\phi}^2 - \frac{\alpha^2}{2L_{\text{osc}}} \phi^2 - \alpha^2 C_{\text{int}} \dot{\varphi} \dot{\phi}. \quad (24)$$

The simple capacitance renormalizations $C \rightarrow C + C_{\text{int}}$ and $C_{\text{osc}} \rightarrow C_{\text{osc}} + C_{\text{int}}$ present in (21) and (22) have been ignored here but can easily be accounted for below. The velocity-velocity coupling in (24) will lead to a $\sigma_J^y \sigma_{\text{osc}}^y$ interaction term in the Hamiltonian.

The canonical momenta are

$$p_\varphi = \alpha^2 C \dot{\varphi} - \alpha^2 C_{\text{int}} \dot{\phi} \quad \text{and} \quad p_\phi = \alpha^2 C_{\text{osc}} \dot{\phi} - \alpha^2 C_{\text{int}} \dot{\varphi}. \quad (25)$$

The velocities in terms of these momenta are

$$\dot{\varphi} = \frac{C_{\text{osc}} p_{\varphi} + C_{\text{int}} p_{\phi}}{\alpha^2 (C C_{\text{osc}} - C_{\text{int}}^2)} \quad \text{and} \quad \dot{\phi} = \frac{C_{\text{int}} p_{\varphi} + C p_{\phi}}{\alpha^2 (C C_{\text{osc}} - C_{\text{int}}^2)}. \quad (26)$$

Quantization then leads to

$$H = p_{\varphi} \dot{\varphi} + p_{\phi} \dot{\phi} - L = H_{\varphi} + H_{\phi} + \delta H, \quad (27)$$

where $[\varphi, p_{\varphi}] = i\hbar$, $[\phi, p_{\phi}] = i\hbar$, and

$$\delta H = \frac{C_{\text{int}}}{\alpha^2 (C C_{\text{osc}} - C_{\text{int}}^2)} p_{\varphi} p_{\phi}. \quad (28)$$

Typically $C_{\text{int}} \ll \sqrt{C C_{\text{osc}}}$, allowing the C_{int}^2 in the denominator to be dropped. Furthermore,

$$H_{\varphi} = E_c N^2 - E_J \cos \varphi + \frac{\alpha^2}{2L} (\varphi - 2\pi x)^2 \quad (29)$$

and

$$H_{\phi} = \frac{p_{\phi}^2}{2\alpha^2 C_{\text{osc}}} + \frac{\alpha^2 \phi^2}{2L_{\text{osc}}}. \quad (30)$$

The kinetic energy in H_{ϕ} is electrical in origin and the potential energy is magnetic. The strength of quantum fluctuations is characterized by the dimensionless quantity

$$\ell_{\phi} \equiv \sqrt{\frac{\hbar}{\alpha^2 C_{\text{osc}} \omega_{\text{osc}}}}. \quad (31)$$

Finally, I simplify (28) by projecting the squid and oscillator into their $\{|0\rangle, |1\rangle\}$ subspaces. Then

$$p_{\varphi} \rightarrow \frac{\hbar \varphi_{01} \epsilon}{2E_c} \sigma^y, \quad (32)$$

where $\varphi_{01} \equiv \langle 0|\varphi|1\rangle$ is the JJ dipole moment and $\epsilon \equiv \epsilon_1 - \epsilon_0$ is the qubit level spacing (both calculated in the absence of coupling to the oscillator). To obtain this result I have used the identity $[\varphi, H_{\varphi}] = 2iE_c N$, allowing us to relate momentum and dipole matrix elements. The oscillator momentum operator projects similarly,

$$p_{\phi} \rightarrow \frac{\hbar}{\sqrt{2} \ell_{\phi}} \sigma^y, \quad (33)$$

Then we obtain [dropping the C_{int}^2 in the denominator of (28)]

$$\delta H = g \sigma_J^y \sigma_{\text{osc}}^y, \quad (\text{parallel circuit}) \quad (34)$$

where

$$g = \frac{\hbar^2 C_{\text{int}} \varphi_{01} \epsilon}{2\sqrt{2} \alpha^2 C C_{\text{osc}} E_c \ell_{\phi}} = \frac{1}{2} \left(\frac{C_{\text{int}}}{C_{\text{osc}}} \right) \left(\frac{\sqrt{2} \varphi_{01}}{\ell_{\phi}} \right) \epsilon. \quad (35)$$

Note that in the harmonic junction limit, $\varphi_{01} = \ell_{\varphi}/\sqrt{2}$, with ℓ_{φ} the width of the wave functions in the junction.

3.2 JJ coupled to series LC oscillator

Referring to Fig. 6, the equations of motion are

$$\alpha^2 C \ddot{\varphi} + E_J \sin \varphi + \frac{\alpha^2}{L} \varphi - \frac{2\pi\alpha^2 x}{L} = -\alpha \dot{q} \quad (36)$$

and, assuming $C_{\text{int}} \neq 0$,

$$L_{\text{osc}} \ddot{q} + \frac{q}{C'_{\text{osc}}} = \alpha \dot{\varphi}, \quad (37)$$

where $C'_{\text{osc}} \equiv (C_{\text{osc}}^{-1} + C_{\text{int}}^{-1})^{-1}$. Note that the capacitance C_{int} does not enter the cross-coupling terms on the right-hand-sides of (36) and (37). This is an indication that the qubit-oscillator coupling in this system is nonperturbative: The limit $C_{\text{int}} \rightarrow 0$ differs from the case $C_{\text{int}} = 0$, and there is no small parameter associated with the interaction. A Lagrangian leading to (36) and (37) is⁴

$$L = \frac{\alpha^2 C}{2} \dot{\varphi}^2 + E_J \cos \varphi - \frac{\alpha^2}{2L} (\varphi - 2\pi x)^2 + \frac{L_{\text{osc}}}{2} \dot{q}^2 - \frac{1}{2C'_{\text{osc}}} q^2 + \alpha \dot{\varphi} q. \quad (38)$$

The canonical momenta are

$$p_{\varphi} = \alpha^2 C \dot{\varphi} + \alpha q \quad \text{and} \quad p_q = L_{\text{osc}} \dot{q}, \quad (39)$$

leading to the quantum Hamiltonian

$$H = \frac{(p_{\varphi} - \alpha q)^2}{2\alpha^2 C} - E_J \cos \varphi + \frac{\alpha^2}{2L} (\varphi - 2\pi x)^2 + \frac{p_q^2}{2L_{\text{osc}}} + \frac{q^2}{2C'_{\text{osc}}}. \quad (40)$$

The squid sees the oscillator as a source of vector potential $A \propto \alpha q$, whose time derivative describes an effective electric field. Noting that the ‘‘diamagnetic’’ A^2 term serves to further decrease the oscillator capacitance, I obtain

$$H = H_{\varphi} + H_q + \delta H, \quad (41)$$

where H_q is the oscillator Hamiltonian

$$H_q = \frac{p_q^2}{2L_{\text{osc}}} + \frac{q^2}{2C'_{\text{osc}}} = \hbar\omega_{\text{osc}} \left(a^{\dagger} a + \frac{1}{2} \right), \quad \omega_{\text{osc}} \equiv \sqrt{\frac{1}{L_{\text{osc}} C'_{\text{osc}}}}, \quad (42)$$

where

$$C'_{\text{osc}} \equiv (C_{\text{osc}}^{-1} + C^{-1} + C_{\text{int}}^{-1})^{-1}, \quad (43)$$

and

$$\delta H = -\frac{p_{\varphi} q}{\alpha C} \quad (44)$$

is the qubit-oscillator interaction.

In the $\{|0\rangle, |1\rangle\}$ subspace of the series oscillator,

$$q \rightarrow \frac{\ell_q}{\sqrt{2}} \sigma^x, \quad (45)$$

⁴An alternative form for L has an interaction term $\delta L = -\alpha \varphi \dot{q}$.

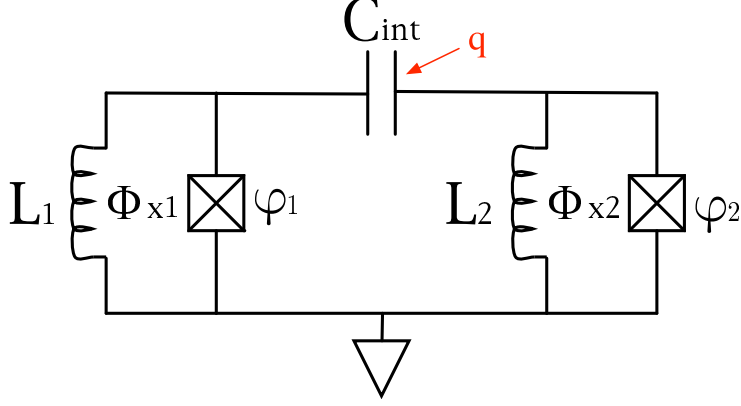


Figure 7: Capacitively coupled qubits.

where

$$\ell_q \equiv \sqrt{\frac{\hbar}{L_{\text{osc}} \omega_{\text{osc}}}}. \quad (46)$$

Then we have

$$\delta H = -g \sigma_J^y \sigma_{\text{osc}}^x, \quad (\text{series circuit}) \quad (47)$$

where

$$g = \frac{\varphi_{01} \ell_q}{2\sqrt{2} e} \epsilon. \quad (48)$$

Note that there is no factor of $C_{\text{int}}/C_{\text{osc}}$ here. The coupling constant (48) is small (much less than the qubit level spacing ϵ) only if the quantum fluctuations in both the squid and oscillator are small.

3.3 Relation to capacitively coupled qubits

It is useful to compare the result for the qubit–parallel-LC system to a pair of capacitively coupled qubits. Referring to Fig. 7, the equations of motion are

$$\alpha^2 C'_1 \ddot{\varphi}_1 + E_{J1} \sin \varphi_1 + \frac{\alpha^2}{L_1} (\varphi_1 - 2\pi x_1) = \alpha^2 C_{\text{int}} \ddot{\varphi}_2 \quad (49)$$

$$\alpha^2 C'_2 \ddot{\varphi}_2 + E_{J2} \sin \varphi_2 + \frac{\alpha^2}{L_2} (\varphi_2 - 2\pi x_2) = \alpha^2 C_{\text{int}} \ddot{\varphi}_1, \quad (50)$$

where

$$C'_i \equiv C_i + C_{\text{int}}, \quad (i = 1, 2). \quad (51)$$

The Lagrangian for the coupled system is

$$L = \sum_i \left[\frac{\alpha^2 C'_i}{2} \dot{\varphi}_i^2 + E_{Ji} \cos \varphi_i - \frac{\alpha^2}{2L_i} (\varphi_i - 2\pi x_i)^2 \right] - \alpha C_{\text{int}} \dot{\varphi}_1 \dot{\varphi}_2, \quad (52)$$

leading to the Hamiltonian

$$H = \frac{C'_2 p_1^2 + C'_1 p_2^2 + 2C_{\text{int}} p_1 p_2}{2\alpha^2 (C'_1 C'_2 - C_{\text{int}}^2)}. \quad (53)$$

In the 2-qubit subspace the interaction Hamiltonian is $\delta H = g\sigma_1^y\sigma_2^y$, where

$$g = \frac{C_{\text{int}}\varphi_{01}^{(1)}\varphi_{01}^{(2)}\epsilon^{(1)}\epsilon^{(2)}}{4e^2} = \frac{1}{2}\frac{C_{\text{int}}}{\sqrt{C_1C_2}}\left[\left(\frac{\sqrt{2}\varphi_{01}^{(1)}}{\ell^{(1)}}\right)\left(\frac{\sqrt{2}\varphi_{01}^{(2)}}{\ell^{(2)}}\right)\sqrt{\frac{\epsilon^{(1)}}{\hbar\omega^{(1)}}}\sqrt{\frac{\epsilon^{(2)}}{\hbar\omega^{(2)}}}\right]\sqrt{\epsilon^{(1)}\epsilon^{(2)}}. \quad (54)$$

Here ω is the classical oscillation frequency of the JJ, and $\ell \equiv \sqrt{2E_c/\hbar\omega}$ is the associated wave function width. The factor in square brackets is unity for JJs in the harmonic limit. If we now assume identical junctions, with the second biased in the harmonic regime so that it is similar to an oscillator, then after some rearrangement we obtain

$$g = \frac{1}{2}\left(\frac{C_{\text{int}}}{C}\right)\left(\frac{\sqrt{2}\varphi_{01}^{(1)}}{\ell^{(2)}}\right)\epsilon^{(1)}, \quad (55)$$

which corresponds precisely to (35).

4 Qubit coupled to electromagnetic resonator

I now consider an rf squid coupled to a coplanar waveguide resonator. The charge qubit case has been addressed by Blais *et al.* [5]. A simplified form of the system layout is shown in Fig. 8. The squid has been discussed in Sec. 3. The coplanar waveguide resonator consists of a conducting strip of length d and width w , capacitively coupled to rf transmission lines. Fig. 9 shows a hybrid circuit model for the system, where the resonator is described at the level of microscopic electrodynamics and the squid is in the usual lumped circuit limit. The geometry considered also allows for the position x_0 of the qubit along the resonator to vary; $x_0 = 0$ is the case shown in Fig. 8.

The system Hamiltonian is derived in two different ways. The simplest is to treat the resonator in the continuum limit, the approach followed in Sec. 4.2. However, for numerical simulations the discrete LC ladder model of the resonator used in Sec. 4.3 is preferable. Both models lead to the Hamiltonian and coupling constant given below in (56) and (57).

4.1 Summary of results and mapping to qubit-oscillator

I will show below that after projection into the qubit subspace of the squid and the vacuum and 1-photon subspace of the fundamental mode of the resonator, the interaction Hamiltonian for the system shown in Fig. 9 is

$$\delta H = g\sigma_\varphi^y\sigma_\phi^y, \quad (56)$$

where

$$g \equiv \cos\left(\frac{\pi x_0}{d}\right)\frac{C_{\text{int}}\varphi_{01}\sqrt{\hbar\omega_{\text{res}}}}{2e\sqrt{Cd}}\epsilon. \quad (57)$$

The subscripts φ and ϕ refer to the JJ phase and oscillator node-flux degrees of freedom, respectively (it will be necessary to distinguish between matrix representations of the oscillator variables written in different bases). In addition, C_{int} is the coupling capacitance, φ_{01} is the squid dipole moment,

$$\omega_{\text{res}} = \frac{\pi v}{d} \quad (58)$$

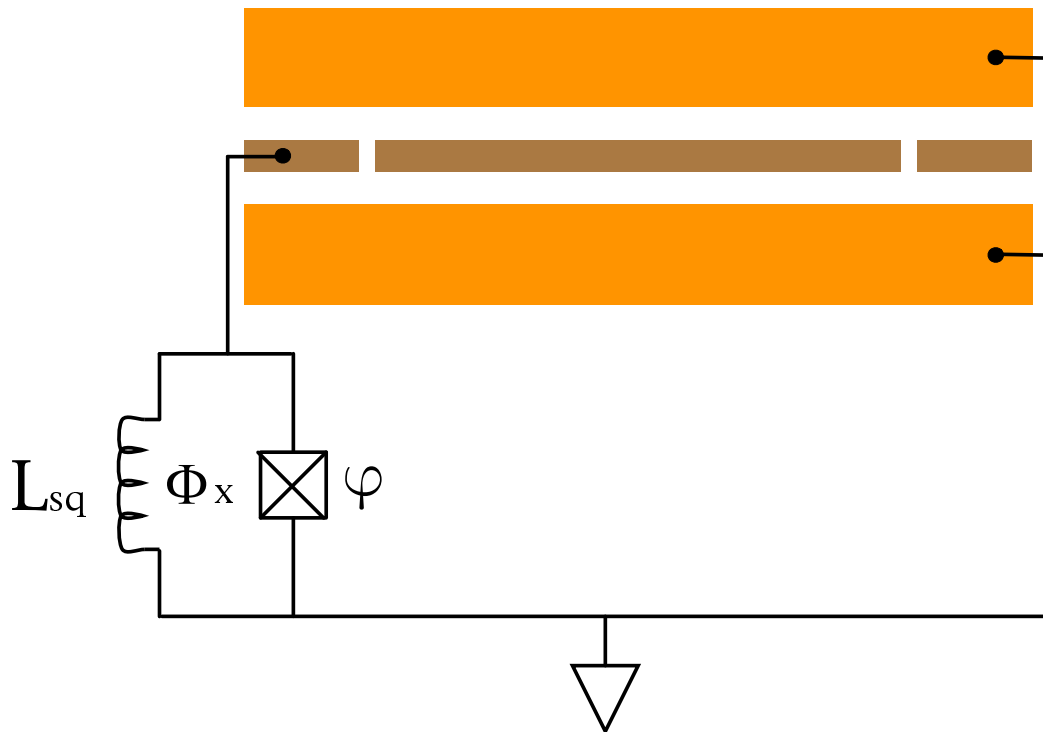


Figure 8: Superconducting qubit coupled to coplanar waveguide resonator. The inner regions represent the resonator and capacitively coupled rf transmission lines. The wide outer regions are ground planes.

is the angular frequency of the fundamental mode of the resonator, written in terms of the transmission line wave speed

$$v \equiv \sqrt{\frac{1}{\mathcal{L}\mathcal{C}}}, \quad (59)$$

\mathcal{L} and \mathcal{C} are the inductance and capacitance per unit length of the coplanar waveguide, d is the resonator length, and ϵ is the qubit energy level spacing. On resonance we have $\epsilon = \hbar\omega_{\text{res}}$.

The coupling constant quoted in (57) assumes two conditions on the allowed values of C_{int} . First, C_{int} must be much smaller than the JJ capacitance C . In particular, the calculation is done to leading nontrivial order in the parameter C_{int}/C . This is the usual condition for weak coupling, and it is easily satisfied experimentally. The second condition on C_{int} is more restrictive and arises because of the modification of the resonator modes themselves by the attached squid. This modification depends on both C_{int} and on the size of the attachment point of the lumped part of the circuit to the microscopic continuous part, and is denoted by b in Fig. 9. In the design of Fig. 8, b is just the resonator width w . The condition that the qubit couples to modes of the *isolated* resonator requires that C_{int} be much smaller than

$$C^* \equiv Cb, \quad (60)$$

which can be interpreted as the capacitance “under” the attachment wire. If C_{int} is not much smaller than C^* , then the resonator modes the qubit couple to are themselves nontrivially modified by the coupling to the squid, and the coupling constant (57) is modified.

The Hamiltonian (56) can be mapped to a qubit coupled to a single parallel LC oscillator.

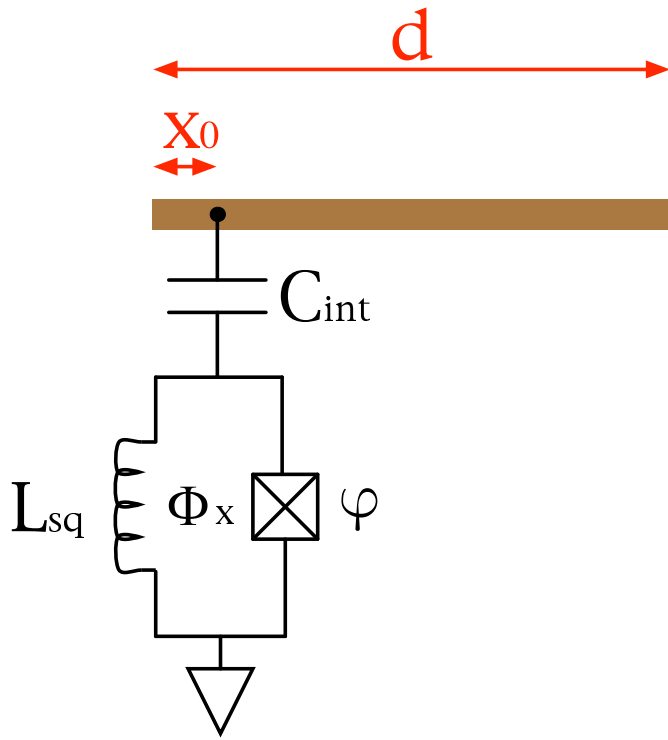


Figure 9: Hybrid circuit model used to construct Hamiltonian. The qubit is coupled via a capacitance C_{int} to a resonator of length d at a distance x_0 from the end; the layout of Fig. 8 corresponds to $x_0 = 0$. The width of the resonator is w . The ground planes are not shown and the figure is not to scale. Coupling to transmission lines is ignored. The diameter of the wire connecting C_{int} to the resonator also enters the model and is denoted by b .

To do this, define an effective oscillator inductance and capacitance

$$L_{\text{eff}} \equiv \frac{2}{\pi^2} \mathcal{L}d \quad \text{and} \quad C_{\text{eff}} \equiv \frac{1}{2} \mathcal{C}d. \quad (61)$$

Note that the oscillator frequency

$$\sqrt{\frac{1}{L_{\text{eff}}C_{\text{eff}}}} \quad (62)$$

implied by these effective quantities is equal to the actual fundamental mode frequency (58), as expected. In terms of L_{eff} and C_{eff} we can write (57) as

$$g = \frac{\cos(\frac{\pi x_0}{d})}{2} \left(\frac{C_{\text{int}}}{C_{\text{eff}}} \right) \left(\frac{\sqrt{2} \varphi_{01}}{\ell_{\text{eff}}} \right) \epsilon, \quad \text{with} \quad \ell_{\text{eff}} \equiv \sqrt{\frac{\hbar}{\alpha^2 C_{\text{eff}} \omega_{\text{res}}}} = \sqrt{\frac{(\frac{4e^2}{C_{\text{eff}}})}{\hbar \omega_{\text{res}}}}. \quad (63)$$

When $x_0 = 0$, this expression has precisely the form for coupling to a parallel LC oscillator with inductance L_{eff} and capacitance C_{eff} .

The second expression for ℓ_{eff} in (63) emphasizes that it is a dimensionless measure of the electric field energy in an LC oscillator. In the quantum description of a squid coupled to an parallel LC oscillator, the relevant oscillator degree of freedom is a node-flux variable, and in the node-flux representation the kinetic energy term in the Hamiltonian is electric in origin. Thus, ℓ_{eff} is also a dimensionless measure of the quantum zero-point motion in the fundamental mode of the resonator.

4.2 Continuum resonator model

The resonator lies on the x axis with its left end at the origin. Referring to Fig. 9, let $\rho(x, t)$, $I(x, t)$, and $V(x, t)$ be the charge per unit length, the current in the x direction, and the electric potential on the resonator, and let \mathcal{L} and \mathcal{C} be the inductance and capacitance per unit length of the coplanar waveguide.

The equation of motion for an infinite waveguide follows from the inductance equation

$$\partial_x V + \mathcal{L} \partial_t I = 0, \quad (64)$$

the capacitance equation

$$\rho = \mathcal{C} V, \quad (65)$$

and the continuity equation

$$\partial_t \rho + \partial_x I = 0. \quad (66)$$

These lead to the wave equation

$$(\partial_t^2 - v^2 \partial_x^2) \rho = 0, \quad (67)$$

with velocity given in (59). The potential V and current I satisfy identical wave equations, but these will not be needed here.

A finite segment of waveguide—a resonator—satisfies the wave equation (67) together with the boundary conditions that $I = 0$ at the ends. Using (64), we see that these boundary conditions require $\partial_x \rho$ (or $\partial_x V$) to vanish at the ends, leading to charge (or voltage) antinodes there. I also assume that the resonator carries no net charge, so that

$$\int_0^d dx \rho = 0. \quad (68)$$

The charge density eigenmodes are

$$f_n(x) \equiv \sqrt{\frac{2}{d}} \cos\left(\frac{n\pi x}{d}\right), \quad n = 1, 2, 3, \dots, \quad (69)$$

the $n = 0$ mode excluded because of the charge neutrality condition (68). These satisfy the orthonormality condition

$$\int_0^d dx f_n f_{n'} = \delta_{nn'}. \quad (70)$$

The mode angular frequencies are

$$\omega_n = \frac{n\pi v}{d}. \quad (71)$$

Below we will primarily be interested in the fundamental mode, $n = 1$, with the frequency given in (58).

To derive a Hamiltonian for the system shown in Fig. 9, it will be necessary to account for the finite width b of the wire connecting the resonator to the coupling capacitor. In the actual device, b is equal to the width w of the waveguide, but in future designs these may differ. The finite width of the wire smears the squid-resonator interaction over a region of size b . I account for this by introducing a broadened delta function $\Delta(x)$ of width b , satisfying

$$\int_0^d dx \Delta(x - x_0) = 1, \quad b < x_0 < d - b. \quad (72)$$

The actual shape of Δ is determined by the microscopic current density at the squid-resonator junction. However, for definiteness I assume a square shape

$$\Delta(x) \equiv \begin{cases} \frac{1}{b} & |x| \leq \frac{b}{2} \\ 0 & |x| > \frac{b}{2} \end{cases}. \quad (73)$$

Because the wavelengths of the modes of interest here are much larger than b , the detailed shape of $\Delta(x)$ should be irrelevant as long as $\Delta(x)$ is everywhere finite. In particular, it is not possible to take the $b \rightarrow 0$ limit, where $\Delta(x)$ becomes a delta function, as $\delta(0)$ diverges.

To find the equations of motion for the system of Fig. 9, let q_{int} be the charge induced on the upper (resonator side) plate of the coupling capacitor. We take the fundamental degrees of freedom of the circuit to be the JJ coordinate φ and the resonator density field $\rho(x)$, suppressing the time argument in all quantities when not necessary. In terms of these degrees of freedom,

$$q_{\text{int}} = C_{\text{int}} \left[\frac{\bar{\rho}(x_0)}{\mathcal{C}} - \alpha \dot{\varphi} \right], \quad (74)$$

where

$$\bar{f}(x) \equiv \int dx' \Delta(x' - x) f(x') \quad (75)$$

denotes the average of a quantity $f(x)$ over a width b , and

$$\alpha \equiv \frac{\hbar}{2e}. \quad (76)$$

The equation of motion for φ is

$$\alpha^2 C \ddot{\varphi} + E_J \sin \varphi + \frac{\alpha^2}{L_{\text{sq}}} \left(\varphi - 2\pi \frac{\Phi_x}{\Phi_{\text{sc}}} \right) = \alpha \dot{q}_{\text{int}}, \quad (77)$$

where

$$\Phi_{\text{sc}} \equiv \frac{hc}{2e} \quad (78)$$

is the superconducting flux quantum and Φ_x is the external magnetic flux. Then

$$\alpha^2 C' \ddot{\varphi} + E_J \sin \varphi + \frac{\alpha^2}{L_{\text{sq}}} \left(\varphi - 2\pi \frac{\Phi_x}{\Phi_{\text{sc}}} \right) = \alpha \frac{C_{\text{int}}}{\mathcal{C}} \partial_t \bar{\rho}(x_0), \quad C' \equiv C + C_{\text{int}}. \quad (79)$$

The equation of motion for the charge density can be obtained by modifying the continuity equation (66) to account for the current drain to the squid. It will be necessary to account for the finite width of the wire connecting the resonator to the coupling capacitor. Then

$$\partial_t \rho + \partial_x I = -\Delta(x - x_0) \dot{q}_{\text{int}}. \quad (80)$$

The sign on the right-hand-side of (80) assures that the resonator sees the current \dot{q}_{int} flowing downward through the coupling capacitor as a current sink. Combining (80) with (64) and (65) leads to

$$[\mathcal{C}'(x) \partial_t^2 - \frac{1}{\mathcal{L}} \partial_x^2] \rho = \alpha C_{\text{int}} \mathcal{C} \Delta(x - x_0) \ddot{\varphi}, \quad \mathcal{C}'(x) \equiv \mathcal{C} + \Delta(x - x_0) C_{\text{int}}. \quad (81)$$

To obtain (81) I have used the fact that (for the modes of interest) ρ is slowly varying on the scale b , so that $\Delta(x - x_0) \bar{\rho}(x_0) \approx \Delta(x - x_0) \rho(x)$.

As with our earlier investigation of a squid capacitively coupled to a parallel LC oscillator, there is no time-local Lagrangian that gives the equations of motion (79) and (81). To proceed, make a transformation from ρ to a dimensionless node-flux *field*

$$\phi(x, t) \equiv \frac{1}{\alpha \mathcal{C}} \int_{-\infty}^t dt' \rho(x, t') \quad (82)$$

and integrate the equation resulting from (81) over time. This leads to the set of coupled equations

$$\alpha^2 C' \ddot{\varphi} + E_J \sin \varphi + \frac{\alpha^2}{L_{\text{sq}}} \left(\varphi - 2\pi \frac{\Phi_x}{\Phi_{\text{sc}}} \right) = \alpha^2 C_{\text{int}} \partial_t^2 \bar{\phi}(x_0) \quad (83)$$

and

$$\alpha^2 (\mathcal{C}' \partial_t^2 - \frac{1}{\mathcal{L}} \partial_x^2) \phi = \alpha^2 C_{\text{int}} \Delta(x - x_0) \ddot{\varphi}, \quad (84)$$

dropping an arbitrary constant of integration. A Lagrangian for the coupled system is

$$\begin{aligned} L = & \frac{\alpha^2 C'}{2} \dot{\varphi}^2 + E_J \cos \varphi - \frac{\alpha^2}{2L_{\text{sq}}} \left(\varphi - 2\pi \frac{\Phi_x}{\Phi_{\text{sc}}} \right)^2 \\ & + \int_0^d dx \left[\frac{\alpha^2 C'}{2} (\partial_t \phi)^2 - \frac{\alpha^2}{2\mathcal{L}} (\partial_x \phi)^2 \right] - \int_0^d dx \alpha^2 C_{\text{int}} \dot{\varphi} \Delta(x - x_0) \partial_t \phi(x). \end{aligned} \quad (85)$$

The canonical momenta are

$$p = \alpha^2 C' \dot{\phi} - \alpha^2 C_{\text{int}} \partial_t \bar{\phi}(x_0) \quad (86)$$

and

$$\Pi(x) = \alpha^2 C'(x) \partial_t \phi(x) - \alpha^2 C_{\text{int}} \dot{\phi} \Delta(x - x_0). \quad (87)$$

Note that the resonator momentum density $\Pi(x)$ is a field; it depends on x . The velocities in terms of these momenta are

$$\dot{\phi} = \frac{C'(x_0) p + C_{\text{int}} \bar{\Pi}(x_0)}{\alpha^2 [C' C'(x_0) - C_{\text{int}}^2 \Delta(0)]} \quad (88)$$

and

$$\partial_t \phi(x) = \frac{\Pi(x)}{\alpha^2 C'(x)} + \frac{C_{\text{int}} [C'(x_0) p + C_{\text{int}} \bar{\Pi}(x_0)] \Delta(x - x_0)}{\alpha^2 C'(x) [C' C'(x_0) - C_{\text{int}}^2 \Delta(0)]}. \quad (89)$$

The Hamiltonian is

$$H = p \dot{\phi} + \int dx \Pi \partial_t \phi - L = H_\varphi + H_\phi + \delta H, \quad (90)$$

where

$$H_\varphi \equiv \frac{C'(x_0) p^2}{2\alpha^2 [C' C'(x_0) - C_{\text{int}}^2 \Delta(0)]} + U(\varphi), \quad (91)$$

with

$$U(\varphi) \equiv -E_J \cos \varphi + \frac{\alpha^2}{2L_{\text{sq}}} \left(\varphi - 2\pi \frac{\Phi_x}{\Phi_{\text{sc}}} \right)^2, \quad (92)$$

$$H_\phi \equiv \int_0^d dx \left[\frac{\Pi^2}{2\alpha^2 C'} + \frac{\alpha^2 (\partial_x \phi)^2}{2\mathcal{L}} \right] + \frac{C_{\text{int}}^2 [\bar{\Pi}(x_0)]^2}{2\alpha^2 C'(x_0) [C' C'(x_0) - C_{\text{int}}^2 \Delta(0)]}, \quad (93)$$

and

$$\delta H = \frac{C_{\text{int}}}{\alpha^2 [C' C'(x_0) - C_{\text{int}}^2 \Delta(0)]} p \bar{\Pi}(x_0). \quad (94)$$

Quantization leads to the conditions

$$[\varphi, p] = i\hbar \quad \text{and} \quad [\phi(x), \Pi(x')] = i\hbar \delta(x - x'). \quad (95)$$

Next we make two approximations concerning the value of the coupling capacitance C_{int} , namely

$$C_{\text{int}} \ll C \quad \text{and} \quad C_{\text{int}} \ll C^*, \quad (96)$$

where C is the JJ capacitance and C^* is defined in (60). With these assumptions the system Hamiltonian simplifies to

$$H = E_c \mathcal{N}^2 + U(\varphi) + \int dx \mathcal{H}_{\text{res}} + \frac{C_{\text{int}}}{\alpha^2 C} p \Pi(x_0). \quad (97)$$

Here $\mathcal{N} \equiv p/\hbar$ and $E_c \equiv 2e^2/C$. The Hamiltonian density

$$\mathcal{H}_{\text{res}} \equiv \frac{\Pi^2}{2\alpha^2 C} + \frac{\alpha^2 (\partial_x \phi)^2}{2\mathcal{L}} \quad (98)$$

in (97) now describes an isolated resonator. The averaging over $\Pi(x_0)$ in the interaction term has been dropped, as it is assumed that we will use (97) only for resonator modes with wavelengths much larger than b .

The equation of motion resulting from (98) is the operator wave equation $(\partial_t^2 - v^2 \partial_x^2)\phi = 0$, with velocity given in (59). According to (82), the boundary conditions on ϕ are that $\partial_x \phi = 0$ at the resonator ends. Therefore, the charge density eigenfunctions defined in (69) can be used here as a basis in which to expand the node-flux field ϕ and its conjugate momentum, as

$$\phi(x) = \sum_{n=1}^{\infty} \sqrt{\frac{\hbar}{2\alpha^2 \mathcal{C} \omega_n}} f_n(x) [a_n + a_n^\dagger] \quad (99)$$

and

$$\Pi(x) = -i \sum_{n=1}^{\infty} \sqrt{\frac{\alpha^2 \mathcal{C} \hbar \omega_n}{2}} f_n(x) [a_n - a_n^\dagger]. \quad (100)$$

Here a_n and a_n^\dagger are bosonic creation and annihilation operators, and $f_n(x)$ and ω_n are the resonator eigenmodes and frequencies given in (69) and (71). These expansions neglect additive “zero-mode” contributions that are necessary for (99) and (100) to satisfy the second commutation relation in (95), because the eigenfunctions (69) do not themselves form a complete basis, but the zero-mode contributions have no effect here. Using (99) and (100), along with the orthonormality conditions (70) and the additional identity

$$\int_0^d dx f_n'(x) f_{n'}'(x) = \delta_{nn'} \frac{\pi^2 n^2}{d^2}, \quad (101)$$

leads to the expected result

$$H_{\text{res}} \equiv \int dx \mathcal{H}_{\text{res}} = \sum_{n=1}^{\infty} \hbar \omega_n a_n^\dagger a_n. \quad (102)$$

By retaining only the $n = 1$ fundamental-mode term in (100), projecting the squid momentum into the qubit subspace according to

$$p \rightarrow \frac{\hbar \varphi_{01} \epsilon}{2E_c} \sigma^y, \quad (103)$$

and projecting the resonator fundamental mode into the ground and one-photon subspace according to

$$a_1 - a_1^\dagger = i\sigma^y, \quad (104)$$

the interaction term in (97) can now be written as (56) with the coupling constant given in (57).

The $x_0 \rightarrow 0$ limit of (57) has to be taken carefully because of our smearing of the qubit-resonator contact point. The derivation above assumes that $x_0 > b$, so the $x_0 \rightarrow 0$ limit should really be implemented by setting $x_0 \rightarrow b$. However, because $b \ll d$ we can ignore this technicality and let $x_0 = 0$ in (57).

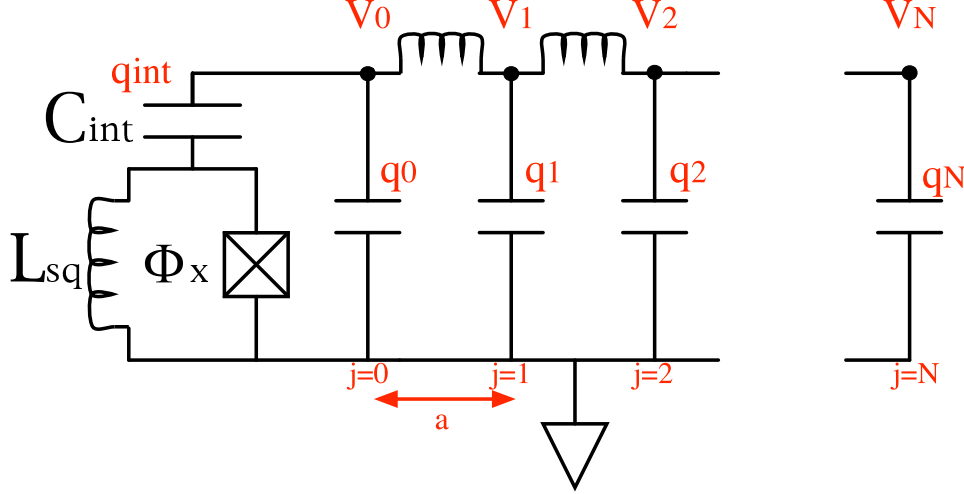


Figure 10: LC network model of the qubit-resonator system. The ladder has N inductors l_0 and $N + 1$ capacitors c_0 .

4.3 LC network resonator model

A discrete network model of the qubit-resonator system is illustrated in Fig. 10. The resonator is modeled as an LC ladder with N inductors l_0 and $N + 1$ capacitors c_0 . The size of each cell is

$$a \equiv \frac{d}{N}, \quad (105)$$

and

$$l_0 = \mathcal{L}a \quad \text{and} \quad c_0 = \mathcal{C}a, \quad (106)$$

with \mathcal{L} and \mathcal{C} the inductance and capacitance per unit length of the physical waveguide. In the continuum limit used below, we let $N \rightarrow \infty$ with d held fixed. This system has N independent resonator degrees of freedom, which I take to be the charges $\{q_1, q_2, \dots, q_N\}$, and one squid degree of freedom φ . The charge q_{int} on the resonator side of the coupling capacitor is fixed by charge neutrality to be

$$q_{\text{int}} = -(q_0 + q_1 + \dots + q_N), \quad (107)$$

and by using the relation $q_{\text{int}} = C_{\text{int}}(\frac{q_0}{c_0} - \alpha\dot{\varphi})$, q_0 can be written in terms of the other degrees of freedom as

$$q_0 = \frac{\alpha C_{\text{int}}\dot{\varphi} - (q_1 + q_2 + \dots + q_N)}{1 + \frac{C_{\text{int}}}{c_0}}. \quad (108)$$

The equation of motion for φ is

$$\alpha^2 C \ddot{\varphi} + E_J \sin \varphi + \frac{\alpha^2}{L_{\text{sq}}} \left(\varphi - 2\pi \frac{\Phi_x}{\Phi_{\text{sc}}} \right) = \alpha \dot{q}_{\text{int}}, \quad (109)$$

or

$$\alpha^2 C' \ddot{\varphi} + E_J \sin \varphi + \frac{\alpha^2}{L_{\text{sq}}} \left(\varphi - 2\pi \frac{\Phi_x}{\Phi_{\text{sc}}} \right) = -\frac{\alpha C_{\text{int}}}{c_0 + C_{\text{int}}} (\dot{q}_1 + \dot{q}_2 + \dots + \dot{q}_N), \quad (110)$$

with

$$C' \equiv C + \frac{C_{\text{int}}}{1 + \frac{C_{\text{int}}}{c_0}}. \quad (111)$$

The equations of motion for the LC ladder are

$$\begin{aligned} l_0 (\ddot{q}_1 + \cdots + \ddot{q}_N) + \frac{q_1}{c_0} + \frac{q_1 + \cdots + q_N}{c_0 + C_{\text{int}}} &= \frac{\alpha C_{\text{int}}}{c_0 + C_{\text{int}}} \dot{\phi}, \\ l_0 (\ddot{q}_2 + \cdots + \ddot{q}_N) + \frac{q_2 - q_1}{c_0} &= 0, \\ l_0 (\ddot{q}_3 + \cdots + \ddot{q}_N) + \frac{q_3 - q_2}{c_0} &= 0, \\ &\vdots \\ l_0 (\ddot{q}_{N-1} + \ddot{q}_N) + \frac{q_{N-1} - q_{N-2}}{c_0} &= 0, \\ l_0 \ddot{q}_N + \frac{q_N - q_{N-1}}{c_0} &= 0. \end{aligned} \quad (112)$$

Next transform to N “polarization” variables u_j , defined by

$$u_j \equiv - \sum_{n=j}^N q_n, \quad j = 1, 2, \dots, N. \quad (113)$$

The inverse relation is

$$q_j = \begin{cases} u_{j+1} - u_j & j < N \\ -u_N & j = N \end{cases}. \quad (114)$$

In particular,

$$\begin{aligned} u_1 &= -(q_1 + q_2 + \cdots + q_N) \\ u_2 &= -(q_2 + q_3 + \cdots + q_N) \\ &\vdots \\ u_{N-1} &= -(q_{N-1} + q_N) \\ u_N &= -q_N \end{aligned} \quad (115)$$

and

$$\begin{aligned} q_1 &= u_2 - u_1 \\ q_2 &= u_3 - u_2 \\ &\vdots \\ q_{N-1} &= u_{N-1} - u_{N-1} \\ q_N &= -u_N. \end{aligned} \quad (116)$$

In the continuum limit, the charge density is

$$\rho(x) = \partial_x u(x), \quad (117)$$

which is why the u_j can be regarded as discrete polarization variables.

In terms of these polarization variables the equations of motion (110) and (112) are

$$\alpha^2 C' \ddot{\varphi} + E_J \sin \varphi + \frac{\alpha^2}{L_{\text{sq}}} \left(\varphi - 2\pi \frac{\Phi_x}{\Phi_{\text{sc}}} \right) = \frac{\alpha C_{\text{int}}}{c_0 + C_{\text{int}}} \dot{u}_1, \quad (118)$$

and

$$\begin{aligned} l_0 \ddot{u}_1 - \frac{u_2 - u_1}{c_0} + \frac{u_1}{c_0 + C_{\text{int}}} &= -\frac{\alpha C_{\text{int}}}{c_0 + C_{\text{int}}} \dot{\varphi}, \\ l_0 \ddot{u}_2 - \frac{u_3 - 2u_2 + u_1}{c_0} &= 0, \\ l_0 \ddot{u}_3 - \frac{u_4 - 2u_3 + u_2}{c_0} &= 0, \\ &\vdots \\ l_0 \ddot{u}_{N-1} - \frac{u_N - 2u_{N-1} + u_{N-2}}{c_0} &= 0, \\ l_0 \ddot{u}_N - \frac{-2u_N + u_{N-1}}{c_0} &= 0. \end{aligned} \quad (119)$$

A Lagrangian for this coupled system of equations is

$$\begin{aligned} L &= \frac{\alpha^2 C'}{2} \dot{\varphi}^2 - U(\varphi) + \sum_{j=1}^N \left(\frac{l_0}{2} \dot{u}_j^2 - \frac{u_j^2}{c_0} \right) + \frac{u_1 u_2 + u_2 u_3 + \cdots + u_{N-1} u_N}{c_0} \\ &\quad - \frac{u_1^2}{2} \left(\frac{1}{c_0 + C_{\text{int}}} - \frac{1}{c_0} \right) - \frac{\alpha C_{\text{int}}}{c_0 + C_{\text{int}}} \dot{\varphi} u_1, \end{aligned} \quad (120)$$

with $U(\varphi)$ defined as in (92). The canonical momenta are

$$p \equiv \frac{\partial L}{\partial \dot{\varphi}} = \alpha^2 C' \dot{\varphi} - \frac{\alpha C_{\text{int}}}{c_0 + C_{\text{int}}} u_1 \quad (121)$$

and

$$p_j \equiv \frac{\partial L}{\partial \dot{u}_j} = l_0 \dot{u}_j, \quad j = 1, 2, \dots, N. \quad (122)$$

Finally, the Hamiltonian is

$$H = H_\varphi + H_u + \delta H, \quad (123)$$

where

$$H_\varphi \equiv \frac{p^2}{2\alpha^2 C'} + U(\varphi), \quad (124)$$

$$H_u \equiv \sum_{j=1}^N \left(\frac{p_j^2}{2l_0} + \frac{u_j^2}{c_0} \right) - \frac{u_1 u_2 + u_2 u_3 + \cdots + u_{N-1} u_N}{c_0} + \frac{u_1^2}{C_1}, \quad (125)$$

with

$$C_1 \equiv \frac{2c_0 C' (c_0 + C_{\text{int}})^2}{C_{\text{int}} [c_0 C_{\text{int}} - (c_0 + C_{\text{int}}) C']} \quad (126)$$

and

$$\delta H \equiv \frac{C_{\text{int}}}{\alpha C' (c_0 + C_{\text{int}})} p u_1. \quad (127)$$

C' is defined in (111).

In addition to the expected squid-resonator interaction term δH , the resonator is itself modified by its coupling to the squid. That coupling results in an additional charging energy u_1^2/C_1 at the position where the squid is attached, modifying the resonator modes. There is also an additional capacitive loading of the squid, as described by the renormalized capacitance C' .

Now we assume

$$C_{\text{int}} \ll C \quad \text{and} \quad C_{\text{int}} \ll c_0. \quad (128)$$

The second condition in (128) is perhaps counterintuitive, because in the continuum limit one would expect c_0 to vanish. However, there is a restriction on how small a can be for the network of Fig. 10 to describe a system with an extended squid-resonator contact region. Because the squid in Fig. 10 is electrically contacted to only a *single* cell of the network, we must require

$$a > b, \quad (129)$$

which implies [see (60) and (106)] the relation $C^* < c_0$. The requirement that $C_{\text{int}} \ll C^*$ therefore leads to

$$C_{\text{int}} \ll C^* < c_0, \quad (130)$$

and hence to the second weak-coupling condition of (128).

With these assumptions the system Hamiltonian simplifies to

$$H = E_c N^2 + U(\varphi) + \sum_{j=1}^N \left(\frac{p_j^2}{2l_0} + \frac{u_j^2}{c_0} \right) - \frac{u_1 u_2 + u_2 u_3 + \cdots + u_{N-1} u_N}{c_0} + \frac{C_{\text{int}}}{\alpha C c_0} p u_1. \quad (131)$$

In this weak coupling limit, the squid couples to the modes of the isolated resonator.

The Lagrangian for an isolated resonator ladder in the polarization representation (120) is

$$L_{\text{res}} = \frac{l_0}{2} \sum_i \dot{u}_i^2 - \frac{1}{2c_0} \sum_{ij} u_i K_{ij} u_j, \quad (132)$$

where

$$K \equiv \begin{pmatrix} 2 & -1 & 0 & 0 & \cdots & 0 & 0 & 0 \\ -1 & 2 & -1 & 0 & \cdots & 0 & 0 & 0 \\ 0 & -1 & 2 & -1 & \cdots & 0 & 0 & 0 \\ & & & \vdots & & & & \\ 0 & 0 & 0 & 0 & \cdots & -1 & 2 & -1 \\ 0 & 0 & 0 & 0 & \cdots & 0 & -1 & 2 \end{pmatrix} \quad (133)$$

is an $N \times N$ matrix that can be recognized as a finite-difference representation of the operator $-\partial_x^2$, truncated in a manner consistent with the continuum boundary conditions (when acting

on an eigenfunction). We wish to transform to a set of uncoupled generalized coordinates ξ_n . Let the $f_i^{(n)}$ [not to be confused with (69)] be the eigenvectors of K ,

$$K f^{(n)} = \lambda^{(n)} f^{(n)}, \quad (134)$$

with n labeling the eigenvectors, the fundamental mode being denoted by $n = 1$. Because K is real and symmetric, its eigenvectors can be chosen to satisfy

$$\sum_i f_i^{(n)} f_i^{(n')} = \delta_{nn'} \quad \text{and} \quad \sum_n f_i^{(n)} f_j^{(n)} = \delta_{ij}. \quad (135)$$

Now we expand the polarization vector in this basis,

$$u_i = \sum_n \xi_n f_i^{(n)}, \quad (136)$$

and obtain

$$L_{\text{res}} = \sum_n \left(\frac{l_0}{2} \dot{\xi}_n^2 - \frac{\omega_n^2}{2c_0} \xi_n^2 \right), \quad (137)$$

which describes independent harmonic oscillators; these are the eigenmodes of the resonator. The resonator frequencies are related to the eigenvalues λ according to

$$\omega = \sqrt{\frac{\lambda}{l_0 c_0}}. \quad (138)$$

The fundamental mode solution of (134) can be found exactly. It is

$$f_i = A \sin\left(\frac{i\pi}{N+1}\right), \quad i = 1, 2, \dots, N. \quad (139)$$

Here

$$A \equiv \left[\sum_{i=1}^N \sin^2\left(\frac{i\pi}{N+1}\right) \right]^{-1/2} \quad (140)$$

is a normalization constant. The lowest eigenvalue is $\lambda = 2[1 - \cos(\frac{\pi}{N+1})]$, and the fundamental-mode frequency is

$$\omega = \frac{2}{\sqrt{l_0 c_0}} \sin\left[\frac{\pi}{2(N+1)}\right]. \quad (141)$$

In the continuum (large N) limit,

$$\omega = \frac{\pi v}{d}, \quad (142)$$

in agreement with (58), and

$$A = \sqrt{\frac{2}{N}}. \quad (143)$$

Keeping only the fundamental mode and quantizing leads to

$$H_{\text{res}} = \frac{p_\xi^2}{2l_0} + \frac{l_0 \omega^2}{2} \xi^2, \quad (144)$$

where p_ξ is the momentum conjugate to ξ . Expanding in bosonic creation and annihilation operators then leads to

$$\xi = \sqrt{\frac{\hbar}{2l_0\omega}} [a + a^\dagger], \quad (145)$$

and

$$H_{\text{res}} = \hbar\omega a^\dagger a. \quad (146)$$

In this representation the interaction is

$$\delta H = \frac{C_{\text{int}} f_1}{\alpha C c_0} p \xi, \quad f_1 = A \sin\left(\frac{\pi}{N+1}\right). \quad (147)$$

After projecting the squid momentum into the qubit subspace according to (32), and projecting the resonator fundamental mode into the ground and one-photon subspace according to

$$\xi \rightarrow \sqrt{\frac{\hbar}{2l_0\omega}} \sigma^x, \quad (148)$$

we obtain the interaction

$$\delta H = g \sigma_\varphi^y \sigma_u^x, \quad (149)$$

with a coupling constant g that can be shown to be identical to (57) in the continuum limit.

4.4 Relation between node-flux and polarization representations

The result (149) appears to differ from (56), but these are written in different bases. In (56), the resonator degree of freedom has been expanded in a basis of eigenstates of node-flux, whereas in (149) a basis of polarization eigenstates is used. Because the transformation between node-flux and polarization is nonlocal in time, the connection between these bases is nontrivial.

Before proceeding, it is interesting to note that (149) and (56) are unitarily equivalent: They have the same spectrum and are therefore related by a unitary transformation. From this point of view it is natural to suspect that they are matrix representations of the same operator written in different bases.

To understand the relation between these representations, return to the description of the continuous isolated resonator in the node-flux representation. Keeping only the $n = 1$ fundamental mode terms in (99) and (100), they may be written as

$$\phi(x) = X f_1(x), \quad X \equiv \sqrt{\frac{\hbar}{2\alpha^2 C \omega_{\text{res}}}} [a_1 + a_1^\dagger], \quad (150)$$

and

$$\Pi(x) = P f_1(x), \quad P \equiv -i \sqrt{\frac{\alpha^2 C \hbar \omega_{\text{res}}}{2}} [a_1 - a_1^\dagger], \quad (151)$$

where

$$f_1(x) = \sqrt{\frac{2}{d}} \cos\left(\frac{\pi x}{d}\right). \quad (152)$$

X can be viewed as an operator describing the node-flux amplitude of the resonator fundamental mode, and P is its conjugate momentum. Inserting these projected quantities into

the Hamiltonian density (98) and integrating, leads to a one-dimensional harmonic oscillator Hamiltonian for the fundamental-mode amplitude,

$$H_{\text{res}} = \frac{P^2}{2\alpha^2\mathcal{C}} + \frac{\alpha^2\mathcal{C}\omega_{\text{res}}^2}{2}X^2. \quad (153)$$

In the node-flux representation, the fundamental-mode eigenstates are eigenfunctions of (153),

$$\psi_m(X) = (2^m m! \sqrt{\pi} \ell)^{-1/2} e^{-X^2/2\ell^2} \mathbf{H}_m\left(\frac{X}{\ell}\right), \quad \ell \equiv \sqrt{\frac{\hbar}{\alpha^2\mathcal{C}\omega_{\text{res}}}}, \quad m = 0, 1, 2, 3, \dots, \quad (154)$$

where the \mathbf{H}_m are Hermite polynomials.

For example, consider the matrix representation of the projected charge density operator $\rho(x)$ in this basis. According to (82),

$$\rho(x) = \alpha\mathcal{C}\partial_t\phi(x) = \frac{\Pi(x)}{\alpha} = \frac{f_1(x)}{\alpha}P, \quad (155)$$

so the matrix elements in the basis (154) are

$$\langle m|\rho(x)|m'\rangle = \frac{f_1(x)}{\alpha}\langle m|P|m'\rangle = -i\hbar\frac{f_1(x)}{\alpha}\times\int dX\psi_m\frac{\partial\psi_{m'}}{\partial X} = \sqrt{\frac{\hbar\omega_{\text{res}}\mathcal{C}}{d}}\cos\left(\frac{\pi x}{d}\right)\sigma_{mm'}^y, \quad (156)$$

where we have further projected to the $m = 0, 1$ subspace.

Now let's compute the matrix elements of $\rho(x)$ in the polarization basis. In the continuum limit, (136) leads to

$$u(x) = \xi\sqrt{\frac{2a}{d}}\sin\left(\frac{\pi x}{d}\right), \quad (157)$$

where we have again projected into the fundamental mode. Similar to X , ξ can be viewed as an operator describing the polarization amplitude of the resonator fundamental mode. The resonator Hamiltonian in this representation is (144), and its eigenfunctions are

$$\psi_m(\xi) = (2^m m! \sqrt{\pi} \ell)^{-1/2} e^{-\xi^2/2\ell^2} \mathbf{H}_m\left(\frac{\xi}{\ell}\right), \quad \ell \equiv \sqrt{\frac{\hbar}{l_0\omega_{\text{res}}}}. \quad (158)$$

Then according to (117), the matrix elements of the projected $\rho(x)$ in the basis (158) are

$$\langle m|\rho(x)|m'\rangle = \sqrt{\frac{2a}{d}}\frac{\pi}{d}\cos\left(\frac{\pi x}{d}\right)\times\int d\xi\psi_m\xi\psi_{m'} = \sqrt{\frac{\hbar\omega_{\text{res}}\mathcal{C}}{d}}\cos\left(\frac{\pi x}{d}\right)\sigma_{mm'}^x. \quad (159)$$

Although I have used the same bracket notation in (156) and (159), it is to be understood that the $|m\rangle$ in these expressions refer to different basis functions.

Comparing (156) and (159), we conclude that the matrices σ_ϕ^y and σ_u^x appearing in (149) and (56) represent the same physical resonator operator written in different bases. Either basis can be used, although the choice of a measurement method may single out one as being more convenient.

References

- [1] M. A. Nielsen and I. L. Chuang, *Quantum Computation and Quantum Information* (Cambridge University Press, Cambridge, England, 2000).
- [2] Y. Makhlin, G. Schön, and A. Shnirman, *Quantum-state engineering with Josephson-junction devices*, Rev. Mod. Phys. **73**, 357–400 (2001).
- [3] J. Q. You and F. Nori, *Superconducting circuits and quantum information*, Physics Today, November 2005, p. 42.
- [4] M. R. Geller and A. N. Cleland, *Superconducting qubits coupled to nanoelectromechanical resonators: An architecture for solid-state quantum information processing*, Phys. Rev. A **71**, 32311 (2005).
- [5] A. Blais, R.-S. Huang, A. Wallraff, S. M. Girvin, and R. J. Schoelkopf, *Cavity quantum electrodynamics for superconducting electrical circuits: An architecture for quantum computation*, Phys. Rev. A **69**, 62320 (2004).